

## Phenological Analysis of Brown Rot Blossom Blight of Sweet Cherry Caused by *Monilinia laxa*

L. Tamm, Chr. E. Minder, and W. Flückiger

First and third authors: Institute for Applied Plant Biology, CH-4124 Schönenbuch, Switzerland; and second author: Department for Social and Preventive Medicine, CH-3012 Berne, Switzerland.

This research was funded by grants of the cantons of Aargau, Basellandschaft, Luzern, Schwyz, Solothurn, and Zug.

Accepted for publication 15 December 1994.

### ABSTRACT

Tamm, L., Minder, Chr. E., and Flückiger, W. 1995. Phenological analysis of brown rot blossom blight of sweet cherry caused by *Monilinia laxa*. *Phytopathology* 85:401-408.

The influence of temperature and wetness duration on infection incidence of sweet cherry blossoms by *Monilinia laxa* was determined in controlled environment studies. Potted sweet cherry trees (cv. Star) were inoculated in full bloom ( $5 \times 10^3$  conidia per milliliter), exposed to 0–24 h of wetness duration and incubated at temperatures between 5 and 20°C. The disease incidence increased with longer wetness duration and temperature within the range tested. A nonlinear model was used to describe the infection incidence as a function of temperature and wetness duration. Analytical tools were developed to determine a posteriori the infection

date of blossoms observed in the field, based on the severity of the symptoms of the disease and the climatic conditions. A temperature-dependent physiological time was introduced to account for the influence of temperature on incubation period. An infected blossom passes through several macroscopically distinct stages of symptom severity. The characteristic change of the relative frequencies of the observed symptoms was used as a measure of the time that had elapsed since infection. The developed methods facilitate the analysis of field data in which the influence of climate, phenological stage of the host, and inoculum density on infection incidence can be elucidated.

*Additional keywords:* *Prunus avium*, epidemiology, stage-frequency matrix.

The brown rot fungus *Monilinia laxa* (Aderhold & Ruhland) Honey is an important pathogen on stone fruit in western Europe (3). In most Swiss orchards, *M. laxa* has recently become an important pathogen on sweet cherry *Prunus avium* L. as well

(13,22,25). Little is known about this particular pathosystem since most studies either describe *M. laxa* on different hosts (18,19,26), or deal with *M. fructicola*, which causes similar symptoms (5,6,24). *Monilinia laxa* causes serious economic losses on sweet cherry due to blossom blight, spur blight, and fruit rot (8). In Switzerland, application of two fungicide treatments during flowering and one during early fruit development (2,21) is recommended.

Disease prediction systems based on climatic factors or inoculum thresholds have been developed in many crops to improve disease management (9). These approaches, however, have so far not been widely applied in the control of brown rot. Aspects of the pathosystem, such as influence of climatic factors on infection incidence, have been studied in controlled environments (24), and sources of inoculum and dispersal mechanisms have been identified (7,10,14,15). Yet, attempts to relate the observed disease severity in the field either to climatic conditions or to inoculum density have not provided consistent results (21). Uncertainty in the date of infection is often a major difficulty in interpretation of field data. Analytical tools that integrate climatic conditions, inoculum density, and the phenological stage of the host would lead to an improved analysis of field data and a better understanding of the *M. laxa*-sweet cherry pathosystem.

In this study two methods were developed to improve the analysis of brown rot epidemics. First, the functional response of infection incidence to temperature and wetness duration under controlled conditions was studied. Second, a method to estimate a posteriori the infection date of diseased blossoms was developed, based on the observed symptom severity of diseased sweet cherry blossoms, and measurements of climatic parameters.

## MATERIALS AND METHODS

**Plants.** Sweet cherry trees *Prunus avium* L. of cv. Star (controlled environment studies, validation studies), or cv. Basler Langstieler (validation studies) were used for infection experiments. Sweet cherry produces a large portion of the flower buds on 2-yr-old wood. Branches bearing floral buds (1.4–2.1 cm basal diameter, 50–80 cm in length) were grafted on *P. avium* cv. F12/1 rootstocks. After grafting, trees were potted (5l pots) and kept at 10°C in darkness for 14 days. Bloom was subsequently induced by transferring the plants to a greenhouse (temperature range 12–23°C). Trees bearing at least 100 fully opened blossoms were selected for the experiments.

**Inoculum.** Isolates of *M. laxa* were collected in 1989 in several regions in Switzerland from naturally infected blossoms of sweet cherry. Isolate BL 8 was used in all studies, whereas other isolates (BL 3, BL 9, SO 19, BE 27, and LU 33) were used in the validation experiments. The isolates were maintained in the dark on malt extract agar (2% w/v; Oxoid CM59) at 2°C. A previously described method was used to produce conidia (23). The medium consisted of agar (2% w/v; Oxoid L11), yeast powder extract (0.2% w/v; Oxoid L21) and macerated, frozen apricot (8% w/v). Agar and apricot extract were autoclaved separately. Each petri dish (9.5 cm

diameter, 17.5 ml of medium) was placed without cover into a sterile polyethylene box (100 × 110 × 40 mm) using the cover of the petri dish as a stand. The bottom of the box was filled with a saturated sterile solution of NaCl that kept the relative humidity (RH) at approximately 75%. A mycelial plug of the stock culture was transferred to each dish, the box was sealed with Parafilm, and incubated for 10 days at 15°C with 14 h/day photoperiod at  $45 \mu\text{E m}^{-2}\text{s}^{-1}$ . The conidia were removed from the colonies by adding 5 ml of sterile, deionized water and carefully scraping off the spores with a glass rod. For inoculation, the spore suspension was adjusted with sterile, deionized water to  $5 \times 10^3$  conidia per milliliter with the aid of a hemacytometer. Individual trees were inoculated with an apparatus consisting of a series of three vertically mounted chromatographic sprayers. Blossoms were uniformly inoculated with 100 ml of a fine mist of spore suspension ( $5 \times 10^3$  conidia per milliliter) at  $1.8 \times 10^6 \text{ Pa}$ .

**Disease assessment.** A successful infection of a sweet cherry blossom by *M. laxa* shows a sequence of typical symptoms of the disease. The symptoms of this process were classified and assigned to six stages (Fig. 1): No symptoms (stage 1), petals necrotic (stage 2), calyx necrotic (stage 3), up to 1/3 of pedicel necrotic (stage 4), more than 1/3 but less than all of pedicel necrotic (stage 5), and whole pedicel necrotic (stage 6). The blossoms were observed repeatedly during all infection experiments (see below) and classified according to these stages of the disease. Occasionally, an infection aborted if infected petals or calyx abscised before the pedicel became diseased.

**Controlled environment studies.** Wetness durations were obtained by covering the individual trees (cv. Star) immediately after inoculation with polyethylene bags for 0, 4, 8, 16, or 24 h. The trees were moved to a growth chamber with a constant temperature of 5, 10, 15, or 20°C, a constant RH of  $80 \pm 10\%$  and a 14-h photoperiod ( $200 \mu\text{E m}^{-2}\text{s}^{-2}$ ). The sequence of the temperature treatments was chosen at random. Temperature and RH were monitored between the plants by means of a datalogger (KMS-P, Anton Paar, Graz, Austria). Six trees were assigned to each combination of temperature and wetness duration. The trees were uncovered after the assigned period and continuously incubated for 30 days (5°C), 15 days (10°C), 10 days (15°C), or 8 days (20°C). Disease incidence was assessed for each spur every day after inoculation (15, 20°C), or every other day (5, 10°C). Blossoms were considered infected if petals showed necrotic spots (stage 2).

**Infection experiments.** The method to determine a posteriori the infection date and its confidence interval was validated with a series of four independent infection experiments. Temperature, RH, wetness duration, and rainfall were measured during these

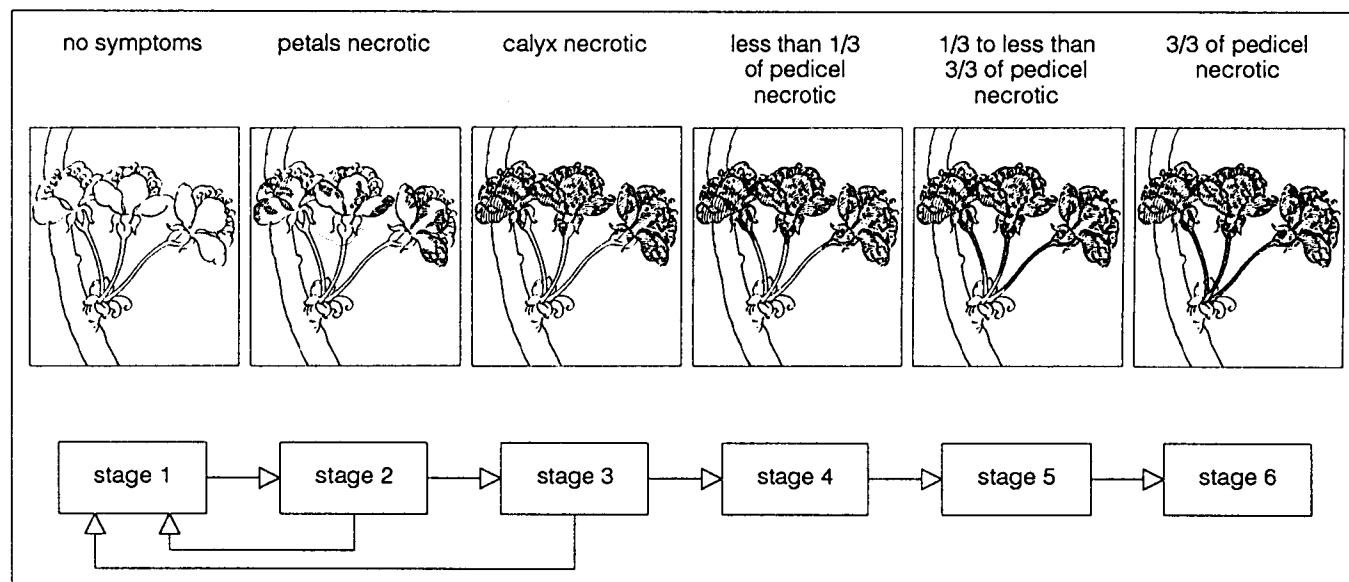


Fig. 1. Schematic diagram of a sweet cherry blossom, displaying subsequent stages of symptoms after infection by *Monilinia laxa*. The symptoms of a diseased blossom were classified to six stages. An infection aborts if infected petals or calyx (stage 2 and 3) abscise early.

experiments by means of an automatic weather station (KMS-P, Anton Paar, Graz, Austria). Plant production and inoculations were conducted as above. The virulence of six isolates of *M. laxa* (BL 3, BL 8, BL 9, SO 19, BE 27, and LU 33) was tested in 1990 on cv. Star (experiment 1) and on cv. Basler Langstieler (experiment 2). Seven replicates per treatment were used in both experiments. After inoculation, the trees were covered with plastic bags for 12 h and subsequently incubated in a greenhouse (temperature range 12–28 °C). Disease incidence was recorded every 2 days. In 1990, 12 3-yr-old potted trees (cv. Star) that were grown outdoors were inoculated at full bloom when flowering naturally occurred (experiment 3). These trees were subsequently exposed to ambient conditions and repeatedly observed. Temperatures recorded ranged from 3 to 27 °C during the observations. In 1992, 12 trees of cv. Langstieler (experiment 4) were inoculated and covered for 4 or 14 h, after inoculation. The trees were subsequently exposed outdoors to ambient conditions and observed for disease every 2–3 days. Temperatures during the observations ranged from 5 to 25 °C.

**Influence of temperature and wetness duration on infection incidence.** The influence of temperature and wetness duration on infection incidence was described with a combination of the Richards model (20) and Analytis's beta model (1). The model has been previously evaluated and was found satisfactory to describe the in vitro germination of conidia of *M. laxa* over a wide range of different conditions (23). Pathogen-dependent parameters ( $T_{min}$ ,  $T_{max}$ , and  $m$ ; see below) determined in vitro were therefore used to describe the infection incidence in vivo as well. The combined model can be written as

$$I(WD, T) = i_{max}(T) \cdot \{1 - (1 - i_0(T)^{1-m}) \cdot \exp(-r(T) \cdot WD)\}^{1/(1-m)} \quad (1)$$

if  $m < 1$

where  $I$  is the estimated proportion of infected blossoms, resulting from an inoculation at temperature  $T$  and wetness duration  $WD$ .  $i_{max}$  is the maximum proportion of infected blossoms,  $i_0$  is the proportion of infected blossoms after 0 h of wetness duration,  $r$  is the rate parameter, and  $m$  is the shape parameter. The model can be simplified if  $m$  is set to 0.9 (23). The parameters  $i_{max}$ ,  $i_0$ , and  $r$  were estimated by nonlinear regression for each temperature treatment. Because the estimates of the maximum proportion of infected blossoms  $i_{max}$  were similar for all temperature treatments,  $i_{max}$  was included as a constant in the final model. The influence of temperature on  $i_0(T)$  and  $r(T)$  was described with the beta function of Analytis (1) that can be written as

$$i_0(T) = \gamma_1 \cdot \phi^{\gamma_2} \cdot (1 - \phi) \quad (2)$$

and

$$r(T) = \rho_1 \cdot \phi^{\rho_2} \cdot (1 - \phi) \quad (3)$$

where

$$\phi = (T - T_{min}) / (T_{max} - T_{min}) \quad (4)$$

where  $T$  is the actual temperature and  $T_{min}$  and  $T_{max}$  are the lower and the upper developmental thresholds.  $T_{min}$  was set to 0 °C and  $T_{max}$  was set to 31 °C, above which mycelial growth ceases. The final nonlinear model describing the infection incidence as influenced by temperature and wetness duration contained the parameters  $i_{max}$ ,  $\gamma_1$ ,  $\gamma_2$ ,  $\rho_1$ , and  $\rho_2$ , which were estimated by nonlinear regression. The model was accepted based on randomness and normality of the residuals, significance of regression coefficients, and  $R^2$ .

**Estimation of date of infection.** A temperature-dependent model was developed to estimate a posteriori the date of infection. The blossoms of a tree represent a cohort of individuals. At observation  $i$ , individual blossoms can be assigned to any of the six develop-

mental stages described above. Starting from the observation  $i=1$  (inoculation), blossoms will potentially proceed from stage 1 (no symptoms) to stage 6 (pedicel entirely necrotic) at observation  $i=n$  if blossoms and pedicel become diseased. Over time, counts of individual blossoms in different stages of symptoms lead to a stage-frequency matrix that is two-dimensional, with  $I$  dates of observations as rows,  $J$  developmental stages as columns, and the frequencies (number of individual blossoms) as matrix elements (see Table 1 for an example). This data structure can be used to calculate the mean lapse of time between infection and the occurrence of each of the six stages of disease severity, i.e., the mean incubation period until a specific symptom occurs. These stage-specific incubation periods were calculated according to the method of Manly (17):

$$F_{i,1} = B_{i-1,1} + f_{i-1,1} \cdot \phi_1 + f_{i-1,2} \cdot \phi_2 + \dots + f_{i-1,J} \cdot \phi_J \quad (5)$$

where

$j$  = index for stages of disease severity;  $j = 1 \dots J = 6$

$f_{i,j}$  = number of individuals in stage  $j$  at sample  $i$ ,

$F_{i,j}$  = number of individuals in stage  $j$  and higher stages in sample  $i$ ,

$\phi_j$  = proportion of individuals remaining in stage  $j$  from one

sample to the next,

$B_{i,j}$  = number of individuals in stage  $j$  or a higher stage that entered stage  $j$  between sample times  $i$  and  $i+1$ .

In our experimental setup, parameter  $B_{i-1,1}$  was known, since no individuals entered the system after inoculation.  $B_{i-1,1}$  is therefore the potential number of successfully infected blossoms, i.e.,  $B_{i-1,1} = F_{i,1}$ . Parameters  $\phi_j$  were estimated by linear least square regression. These parameters range between 0 and 1 by definition. Following Manly (17), the most plausible estimates were searched iteratively: if one or more parameters were estimated higher than 1, the highest parameter was set to 1 and the remaining parameters were re-estimated. From the estimated proportions  $\hat{\phi}_j$  other parameters can be calculated. An estimate of the number of individuals in stage  $j$  or a higher stage that entered stage  $j$  between sample  $i$  and  $i+1$  is

$$\hat{B}_{ij} = F_{i+1,j} - \hat{\phi}_j f_{i,j} - \hat{\phi}_{j+1} f_{i,j+1} - \dots - \hat{\phi}_q f_{i,q} \quad (6)$$

and the total number entering stage  $j$  that survive until a sample time is

$$\hat{M}_j = \sum_{i=1}^{r_j} \hat{B}_{i,j} + F_{1,j} \quad (7)$$

TABLE 1. A stage-frequency matrix, showing observed stage-frequencies for a cohort of 124 sweet cherry blossoms infected by *Monilinia laxa* and incubated at 5 °C<sup>a</sup>

Time (days)	$i$	Stage $j$					
		1	2	3	4	5	6
0	1	124					
2	2	124					
4	3	124					
6	4	124					
8	5	109	15				
10	6	83	41				
12	7	32	91	1			
14	8	19	75	30			
16	9		25	43	32		
18	10		16	30	34	14	
20	11		9	16	18	29	22
22	12			11	13	23	43
24	13				7	26	45

<sup>a</sup>Data represent the frequencies of blossoms of one tree in varied stages of disease severity. The blossoms were inoculated at  $i=1$  and subsequently observed in 2-day intervals. Disease symptoms were assigned to six stages. Stage 1: no symptoms; stage 2: petals necrotic; stage 3: calyx necrotic; stage 4: up to 1/3 of pedicel necrotic; stage 5: more than 1/3 but less than 3/3 of pedicel necrotic; stage 6: whole blossom necrotic. Uninfected blossoms aborted due to lack of pollination.

where  $r_j$  is the sample  $i$ , after which no individuals are found in stage  $j$ .

Finally, the mean duration between inoculation and occurrence of a symptom severity stage (i.e., the mean incubation period of a stage  $j$ ) is calculated by

$$\hat{\mu}_j = \sum_{i=1}^{r_j} i \cdot \hat{B}_{i,j} / \hat{M}_j \quad (8)$$

The distribution of  $\hat{\mu}_j$  is unknown. Therefore, an estimate of the variability of  $\hat{\mu}_j$  was obtained using the jack-knife method (11). Within the same temperature treatments, six sets of  $\hat{\phi}_j$  were calculated, using five out of six replicates for each set.

In order to calibrate the model describing the functional response of the stage-specific incubation period to temperature, additional information of independent in vitro data was used. The modified model of Logan et al (4,16) was well suited to describe the functional response of the in vitro growth of *M. laxa* to temperature (23). The model can be written as

$$R(T) = \begin{cases} p_1 \cdot \{ \exp [p_2 \cdot (T - T_b)] - \exp [p_2 \cdot (T_m - T_b) - \\ p_3 \cdot (T_m - T)] \} - p_4 & \text{if } -2.9 < T \leq 31 \\ 0 & \text{else} \end{cases} \quad (9)$$

where  $R$  is the relative growth,  $T$  the actual temperature (C),  $T_b$  the lowest temperature tested (C), and  $T_m$  the upper developmental threshold (C). Parameters  $p_1$  to  $p_4$  were estimated by nonlinear least square regression techniques ( $p_1 = 0.535$ ,  $p_2 = 0.048$ ,  $p_3 = 0.385$ ,  $p_4 = 0.412$ ,  $T_b = 2.5$  C,  $T_m = 31$  C) (23). Based on this information of the in vitro experiments, it was assumed that relative growth reaches approximately 90% of the maximum growth rate at 20 C (maximum at 24.8 C). In order to transform the relative growth to a time period that represents the mean duration between infection and the occurrence of a stage of disease severity, the model was rescaled using the reciprocal of the original function. The expected stage-specific mean incubation period of symptom severity stage  $j$  as influenced by temperature can then be written as

$$\mu_j(T) = \mu_{\min(20\text{ C})} \cdot 0.9 / R(T) \quad (10)$$

where  $\mu_j(T)$  is the expected mean duration between infection and occurrence of stage  $j$  at temperature  $T$ ,  $\mu_{\min(20\text{ C})}$  is the minimum calculated mean duration between inoculation and

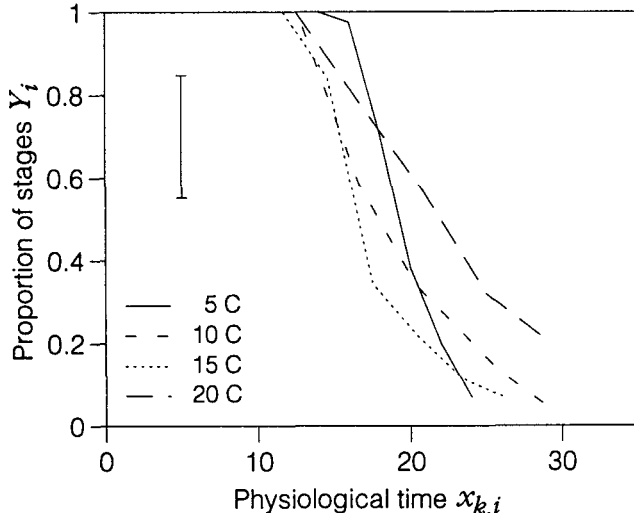


Fig. 2. Definition of the physiological age of a cohort of infected blossoms. Values represent the proportion of disease severity stages  $Y_i$  (equation 12), dependent on physiological time  $x_{k,i}$  (equation 11) at observation  $i$ . Each curve represents the mean of six replicates. Bar indicates the pooled standard deviation.

occurrence of stage  $j$  at 20 C (equation 8), and  $R(T)$  is the relative growth function (equation 9).

The mean incubation periods  $\mu_4$ , that were determined at 5, 10, 15, and 20 C, were visually compared with  $\mu_4(T)$ , the function describing the expected mean incubation period of stage 4 as influenced by temperature (equation 10). The model was tested on data from stage  $j = 4$  (less than 1/3 of pedicel necrotic), because the destruction of the blossom is not reversible at this stage of disease severity, the influence of factors other than temperature (e.g., RH) on the development of the symptoms is still small, and the disease can be accurately determined in the field. Since the calculated  $\mu_4(T)$  showed very close accordance to the observed  $\mu_4$ , it was assumed that the original function (equation 9) was useful to represent the temperature-dependent relative disease progress of *M. laxa* on its host. The modified model of Logan et al (4,16) was therefore used to define a temperature-dependent physiological time scale. This physiological time scale was then used to calculate the accumulated physiological time  $x_k$  after  $k$  hours of development, based on hourly temperature measurements:

$$x_k = \frac{1}{24 \cdot R(5\text{ C})} \cdot (R(T_1) + R(T_2) + \dots + R(T_k)) \quad (11)$$

where  $T_k$  is the mean temperature during the 1-h interval from  $k-1$  to  $k$ , and  $R(T_k)$  denotes the relative growth during that interval (equation 9). Division by  $24 \cdot R(5\text{ C})$  yields a standardized accumulated physiological time: One unit of physiological time equals the development during 1 day at 5 C. For analysis of the infection experiments, accumulation of physiological time  $x_{k,i}$  during the observation period was started at inoculation (i.e.,  $x_{k,i=1} = 0$ ).

During the development of the disease, the proportions of blossoms in each stage of symptoms change over time in a characteristic way. The relative frequencies of blossoms in stages 4–6 were used as a parameter to characterize the physiological age of a cohort of infected blossoms:

$$Y_i = f_{i4} / \sum_{j=4}^{j=6} f_{ij} \quad (12)$$

where  $y_i$  was defined as the number of blossoms in stage  $j = 4$  divided by the total number of blossoms in stages  $j = 4$  to  $j = 6$  at observation  $i$ . The proportions  $Y_i$  were calculated for each of the  $N$  cohorts (i.e., for all temperature treatments and replicates) and standardized to the physiological time  $x_{k,i}$  (equation 11). The ratio  $Y_i$  is undefined until some first individual blossoms reach stage 4 (Fig. 2). Subsequently,  $Y_i$  decreases from 1 to 0 until all blossoms of the cohort either reach stage 5 and 6, or abscise. It was assumed that the relations between proportion  $Y_i$  and accumulated physiological time  $x_{k,i}$  are linear for  $x_{k,i} \leq 25$ . A statistical model of the form

$$Y_{i,n} = c_n + \beta x_{k,i,n} + \epsilon_{i,n} \quad x_{k,i,n} < 25 \quad (13)$$

was fitted to each of the  $N$  cohorts. A model representing all  $N$  cohorts can be written as

$$Y_{i,n} = \hat{\alpha}_n + \hat{\beta} \cdot (x_{k,i,n} - x_\theta) \quad (14)$$

where  $x_\theta$  is chosen ( $x_\theta = 19$ ) such that  $\alpha_n \approx 0.5$  (Fig. 3). In this model, the major source of variation between cohort developments is a shift and the slopes are nearly identical. The median of the  $N$  slope parameters  $\hat{\beta}_n$  was calculated as an estimate of  $\beta$ . Furthermore it was assumed that the  $\hat{\alpha}_1, \hat{\alpha}_2, \dots, \hat{\alpha}_n$  have a normal distribution. Then, the mean  $\alpha_\theta$ , and the variance,  $\sigma^2_\alpha$ , are readily estimated.

The experimentally determined relationship between the observed proportion  $Y_i$  of the symptom severity stages at observation  $i$  and  $x_{k,i}$  (i.e., the accumulated physiological time since infection occurred) can be used to relate the proportion  $Y_i$  of a newly

observed cohort of diseased blossoms to the unknown date of infection  $u'$ . Based on knowledge of  $\hat{x}'_{k,i}$ , an estimate of the unknown infection date  $u'$  and its confidence interval can be obtained.

If a new cohort with an unknown date of infection  $u'$  is observed, the model that describes the linear phase of the relationship between the proportions  $Y_i$  and sample dates  $x'_{k,i}$  can be written as

$$Y_i = \alpha_\theta + \beta(x'_{k,i} - x_\theta - u') + \epsilon_i \quad 0.2 \leq Y_i \leq 1 \quad (15)$$

For each observed  $(Y_i, x'_i)$ , the date of infection  $\hat{u}'_i$  on the physiological time scale is then readily calculated (Fig. 4) using

$$\hat{u}'_i = x'_{k,i} - x_\theta - \frac{Y_i - \hat{\alpha}_\theta}{\hat{\beta}} \quad 0.2 \leq Y_i \leq 1 \quad (16)$$

The upper and lower limits of the 95% confidence interval of

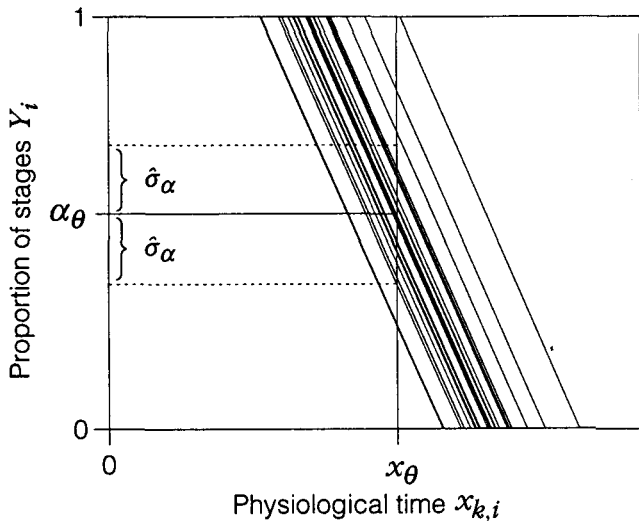


**Fig. 3.** Calibration of a linear model (equations 12–14) describing the development of the proportion of disease severity stages  $Y_i$  (equation 12), dependent on physiological time  $x'_{k,i}$  (equation 11). Each of the lines describes the development of the proportion  $Y_i$  of an individual tree (see text).

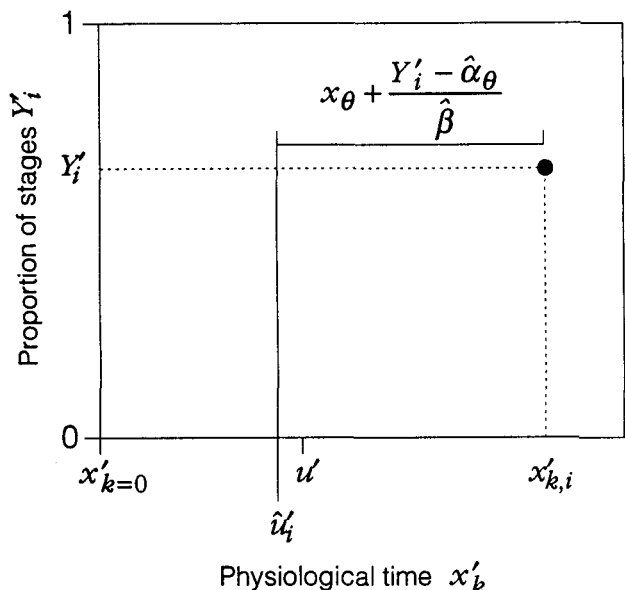


**Fig. 4.** A posteriori determination of the unknown date of infection  $u'$ . The true date of infection  $u'$  is estimated by  $\hat{u}'_i$  (equation 16), based on the proportion of disease severity stages  $Y'_i$  (equation 12) and the accumulated physiological time  $x'_{k,i}$  at observation  $i$  (equation 11).

$\hat{u}'_i$  are estimated by

$$CL(\hat{u}'_i)_{lower/upper} = x'_{k,i} - x_\theta - \frac{Y'_i - (\hat{\alpha}_\theta \pm 2\sqrt{\hat{\sigma}_\alpha^2})}{\hat{\beta}} \quad 0.2 \leq Y'_i \leq 1 \quad (17)$$

If a series of observations of a cohort of infected blossoms yields several valid  $Y'_i$  (i.e.,  $0.2 \leq Y'_i \leq 1$ ) then the mean of all  $\hat{u}'_i$ , and  $CL(\hat{u}'_i)_{lower/upper}$ , respectively, can be used as good estimates of the true infection date  $u'$  and its 95% confidence limits.

**Validation.** The method to estimate the time of infection  $\hat{u}'_i$  and its 95% confidence interval was validated with the four independent data sets described above. The accumulated physiological time  $x'_{k,i}$  was calculated (equation 11) based on hourly means of temperature measurements during the infection experiments. The date of inoculation was set to 0 units of accumulated physiological time (i.e.,  $x'_{k=0,i=1} = 0$ ). Negative values of accumulated

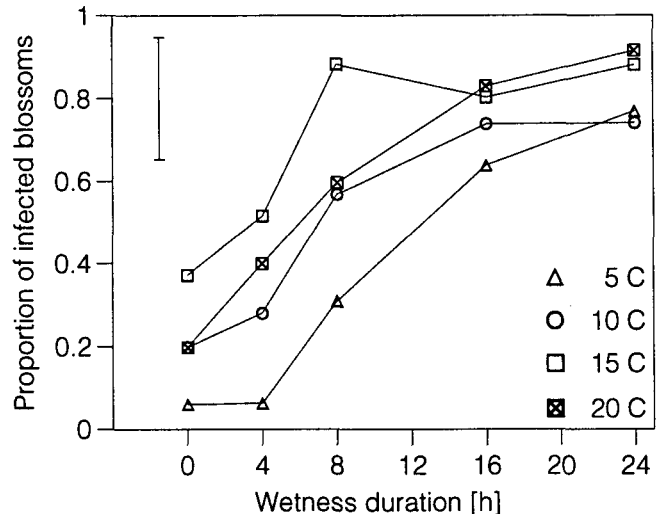


**Fig. 5.** Infection incidence of sweet cherry blossoms infected by *Monilinia laxa* as influenced by temperature and wetness duration. Individual trees were inoculated and subsequently covered for 4, 8, 16, or 24 h to extend wetness duration. Blossoms were considered diseased if petals were necrotic (stage 2). Data points represent the mean of six replicates. Bar indicates the pooled standard deviation.

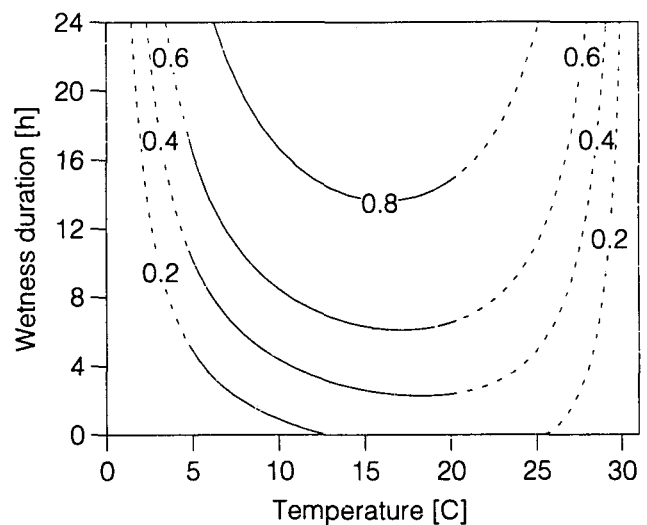


**Fig. 6.** Predicted effect of temperature and wetness duration on disease incidence of sweet cherry blossoms infected by *Monilinia laxa*. The curves represent the two-dimensional projection of the combined model of Richards and Analytis (equations 1–4). Dotted lines indicate the infection incidences outside of the tested range of temperature, as suggested by the model.

physiological time therefore indicate a time prior to the inoculation, and positive values a time later than inoculation. For each data set, the proportion  $Y_i$  and the corresponding accumulated physiological time  $x'_{k,i}$  at the  $i$ th observation were calculated. The infection date  $\hat{u}'$  and its confidence limits were calculated in physiological time units according to equations 16 and 17. The method was considered to yield a successful prediction if the calculated 95% confidence interval contained the true infection date  $u'$ .

All regression analyses were performed with SYSTAT vers. 5.1 (Systat Inc., Evanston, IL).

## RESULTS

**Influence of temperature and wetness duration on infection incidence.** In general, disease severity of infected blossoms increased with longer wetness duration within the range tested. Maximum incidence of diseased blossoms reached up to 90% (Fig. 5). After 24 h of wetness duration, disease incidence reached more than 70%, regardless of the temperature tested. The combined model of Richards (20) and Analytis (1) (equations 1–4) yielded a high coefficient of determination ( $R^2 = 0.74$ ) and highly significant parameter estimates ( $i_{max} = 0.874$ ,  $\gamma_1 = 1.816$ ,  $\gamma_2 = 1.736$ ,  $\rho_1 = 0.728$ ,  $\rho_2 = 0.918$ ;  $p < 0.001$ ). The two-dimensional projection of the model (Fig. 6) represented the observed data satisfactorily for all combinations of temperature and wetness duration and showed no abnormal patterns of the residuals.

**Physiological time.** The mean durations between infection and occurrence of a stage of disease severity (i.e., the mean incubation periods) as influenced by temperature were calculated (equations 5–8) for all stages of the symptoms of disease severity (Table 2). Mean incubation periods of similar developmental stages decreased with higher temperatures. For instance, the mean developmental period of stage 4, i.e., the mean period between infection and occurrence of necrosis of up to 1/3 of the pedicel, was calculated as 15.61 days at 5°C, 8.48 days at 10°C, 5.48 days at 15°C, and 4.06 days at 20°C. The mean incubation period of stage 4  $\hat{\mu}_4$  was compared with the reciprocal nonlinear model of Logan et al (16), which was based on information of the in vitro growth of *M. laxa* (equation 9) and scaled to the mean incubation period of stage 4 at 20°C (equation 10, minimal incubation period obtained  $\hat{\mu}_{4\min}(20^\circ\text{C}) = 3.396$  days). The model showed close accordance to the incubation periods and predicted the medians at 5, 10, and 15°C accurately (Fig. 7). The model was therefore considered satisfactory in order to calculate a temperature-dependent physiological time  $x_k$  (equation 11).

**Physiological age of a cohort of infections.** The use of the proportion  $Y_i$ , the number of blossoms in stage  $j = 4$  divided by the total number of blossoms in stages  $j = 4$  to  $j = 6$ , was well suited to characterize the physiological age of a cohort of infected blossoms at observation  $i$ . These proportions  $Y_i$  (equation 12) were calculated for all temperatures and rescaled to physiological time  $x_k$  (equation 11) (Fig. 2). The  $Y_i$  decreased with increasing physiological time  $x'_{k,i}$  similarly, regardless of tempera-

ture during the disease development. The proportion  $Y_i$  was not defined until at least 12 units of physiological time  $x_k$  had elapsed, i.e., the first blossoms showed necrosis of the pedicel. Subsequently, the ratios decreased linearly until approximately 25 units of physiological time had elapsed. Parameters  $\hat{\beta}$ ,  $\hat{\alpha}_0$ , and  $\hat{\sigma}^2_\alpha$  were estimated (equations 13 and 14) in order to determine the unknown date of infection of a newly observed cohort of infected blossoms  $u'$ , based on the proportion  $Y_i$ , and the physiological time  $x'_{k,i}$  (Fig. 4). The parameters were calculated as  $\hat{\beta} = -0.082$ ,  $\hat{\alpha}_0 = 0.52$ ,  $\hat{\sigma}^2_\alpha = 0.027$ , if  $x_\theta = 19$ .

**Validation.** The method to calculate the confidence interval for the true infection time  $u'$  was validated with the four independent data sets. The most probable infection time  $\hat{u}'$ , and the upper and lower limits of the confidence interval  $CL(\hat{u}')$  were calculated (equations 16 and 17) based on the observed ratios of the stage-frequencies  $Y_i$  and the physiological time  $x'_{k,i}$  (Table 3, Fig. 4). The calculated confidence intervals contained the true infection time  $u'$  in all data sets provided that ratios  $Y_i$  higher than 0.2 were used for calculation. Ratios lower than 0.2 led to spurious results, since the imposed linearity between ratio and physiological time does not hold in the late phase of the development of the symptoms (Fig. 2). The confidence intervals of  $u'$  varied from 79 to 160 h, depending on the temperature during the experiments (Table 3).

## DISCUSSION

Temperature and wetness duration were important environmental factors determining the infection incidence of *M. laxa*

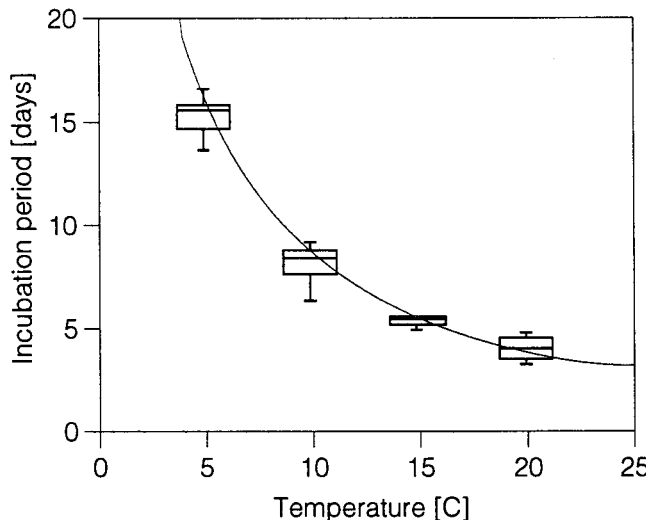


**Fig. 7.** Comparison between the observed  $\hat{\mu}_4$  (boxplots) (equations 5–8) and the expected mean duration  $\hat{\mu}_4(T)$  between inoculation and occurrence of stage 4 of disease severity symptoms (solid line) (equations 9 and 10) at different temperatures. The regression coefficients of the model were estimated based on in vitro growth rates of *M. laxa*.

**TABLE 2.** Influence of temperature on the incubation period  $\hat{\mu}_j$  (i.e., the duration between infection and symptom occurrence) of the different stages of disease severity symptoms of sweet cherry blossoms infected by *Monilinia laxa*<sup>a</sup>

Temperature (°C)	Mean incubation period (days) of stage $j$ <sup>b</sup>						
	$\hat{\mu}_1$	$\hat{\mu}_2$	$\hat{\mu}_3$	$\hat{\mu}_4$	$\hat{\mu}_5$	$\hat{\mu}_6$	
5	0	10.69 [10.44, 11.34]	14.68 [14.32, 14.84]	15.61 [14.67, 15.85]	19.14 [18.81, 19.29]	20.28 [19.75, 20.46]	
10	0	5.56 [5.28, 5.74]	7.30 [7.05, 7.56]	8.48 [7.62, 8.79]	10.55 [9.87, 11.01]	12.36 [11.53, 12.61]	
15	0	2.81 [2.54, 2.92]	4.73 [4.57, 4.91]	5.48 [5.31, 5.59]	6.05 [5.86, 6.10]	6.60 [6.42, 6.85]	
20	0	1.62 [1.23, 2.22]	2.97 [2.73, 3.19]	4.06 [3.65, 4.56]	5.04 [4.83, 5.24]	5.46 [5.32, 5.69]	

<sup>a</sup>Disease severity stages:  $j = 1$ : no symptoms;  $j = 2$ : petals necrotic;  $j = 3$ : calyx necrotic;  $j = 4$ : <1/3 of pedicel necrotic;  $j = 5$ : more than 1/3 but less than 3/3 of pedicel necrotic;  $j = 6$ : whole pedicel necrotic.

<sup>b</sup>Values in brackets indicate the quantiles [ $q_{25\%}$ ,  $q_{75\%}$ ] of the distribution.

on sweet cherry blossoms. *Monilia laxa* is well adapted to the relatively low temperatures during spring. *Monilia laxa* was able to cause infections at temperatures as low as 5°C within very short periods of wetness duration. Wilcox (24) found similar relationships for *M. fructicola* on sour cherry blossoms, although *M. laxa* may be better adapted to low temperature than is *M. fructicola*. In our experiments, infection incidences of up to 40% were observed at 15°C, even if the wetness duration was not extended after inoculation. Presumably, the true wetness durations were partially underestimated: sweet cherry blossoms are clustered, which leads to complex surface structures. Water was withheld in capillary systems within or between the blossoms and, therefore, the wetness duration may have been locally prolonged by up to 4 h. Moreover, the uneven drying process led to a relatively high variability within similar treatments.

The limiting influence of temperature and wetness duration on infection incidence was described with a nonlinear model. The combined model of Richards (20) and Analytis (1) was previously found useful to describe the conidial germination of *M. laxa* in vitro (23). The model also yielded satisfactory results if applied to the controlled environment data presented in this study. The robustness of the model is partly due to its mechanistic structure and, as a result, to its restricted flexibility. The parameters of the model were estimated using information from all treatments and replicates simultaneously. As a consequence, single treatments and outliers had limited influence on the parameter estimates of the final model. The implementation of a priori knowledge, such as the developmental thresholds of the pathogen, considerably improved the reliability of the model predictions at the temperature extremes. Reasonable predictions at low temperatures are important in the sweet cherry pathosystem in Switzerland, because temperatures close to 0°C are common in spring.

A model based on temperature and wetness duration is a useful tool to understand the quantitative influence of these parameters. However, such a model is not likely to predict the disease incidence in the field adequately. It has to be considered as a study of the worst case in which inoculum density is not a limiting factor. In general, the prediction will exceed the observed infection incidence: conidia of *M. laxa* are mostly dispersed by rain splash and wind (8). Some time elapses until a conidium is deposited on a blossom during or after a rain event. The density of conidia decreases exponentially with increasing distance from the source of inoculum (12). The spatial distribution of these sources, i.e., the inoculum density within a tree, therefore influences the time until a conidium lands on a blossom.

The ability to identify the period when blossoms were infected is a prerequisite to interpreting field observations. It facilitates the distinction of the influence of climatic conditions from other factors, such as inoculum density and phenological stage of the host. Our approach to this problem was to relate an observed severity symptom of the disease to the infection date. As a first step, a method to calculate a temperature-dependent physiological time was developed. In a previous study it was shown that the nonlinear model of Logan et al (16) adequately described the relative growth of *M. laxa* in vitro (23). The temperature-dependent period between infection and occurrence of symptoms of the disease severity (i.e., the incubation periods of the symptoms) was used as reference to judge whether the model represented

the influence of temperature in vivo as well, and whether the model was useful to calculate a physiological time. The method of Manly (17) proved to be an effective tool to determine an objective estimate of the mean duration between infection and occurrence of the different stages of symptoms. The precision of the parameter estimates can be considerably increased if replicate matrices are available for computation. In our study, estimates became unstable if less than four replicates were used for calculation. The close accordance of predicted and experimentally obtained incubation periods justified the use of the physiological time units as relevant for the development of *M. laxa* on its host.

As a second step, a method was developed to estimate the physiological age of a cohort of infected blossoms. The method allowed the a posteriori determination of the date of infection and its confidence interval, based on the stages of symptom severity, and calculation of accumulated physiological time. This technique was validated using independent data sets including two sweet cherry cultivars, several isolates of *M. laxa*, and different climatic conditions. The method yielded correct predictions in all cases. For analysis of field data, the determination of the confidence limits of the true date of infection is probably more important than the infection date itself. The confidence interval can be interpreted as the period during which most of the individual blossoms of a cohort become infected. However, the confidence intervals of the validation experiments ranged between 79 and 160 h, dependent on the ambient temperature during the experiments. The conditions during the time interval can be used, as a first approximation to the true date of infection, to analyze the impact of factors that influence the disease incidence, such as the phenological stage of the host, inoculum density, or weather conditions.

A method to determine the time interval when sweet cherry blossoms become infected under field conditions has to be efficient because the observation and classification of a cohort of blossoms in the field is costly. Therefore, the infection interval should be computable based on one or few subsequent observations. The proportion between the frequencies of the stages that cause a necrosis of the pedicel (i.e., stages 4–6) was chosen because these stages can be quickly and accurately determined in the field. The symptoms are easy to recognize and cannot be mistaken for other causes, such as frost damage. The determination of the infection interval is most reliable when the observed ratio is still high (i.e., higher than 0.2). Consequently, a first set of field data should be collected as soon as symptoms of infected pedicels become visible.

The tools presented in this paper will be used to analyze field observations of sweet cherry trees of cv. Star. The analysis of the sweet cherry–*M. laxa* pathosystem elucidates the relative importance of the factors conducive to infection and could finally lead to an improved, threshold-based method for control of brown rot.

#### LITERATURE CITED

1. Analytis, S. 1977. Über die Relation zwischen biologischer Entwicklung und Temperatur bei phytopathogenen Pilzen. *Phytopathol. Z.* 90:64–76.
2. Anonymous. 1993. Pflanzenschutzempfehlungen für den Erwerbs-

TABLE 3. Validation of the a posteriori determination of the date of infection,  $\hat{u}'_i$ , of sweet cherry blossoms by *Monilinia laxa*, based on the ratio of symptom severity stages  $Y'_i$  and physiological time  $x'_{k,i}$ .

Experiment	Cultivar	Infection date		95% confidence limits		Duration of interval
		$u'$	$\hat{u}'$	$\hat{u}_{\text{lower}}$	$\hat{u}_{\text{upper}}$	
1	Star	0	-0.72	-4.95	3.26	96 h
2	BL <sup>b</sup>	0	-0.26	-4.49	3.72	91 h
3	Star	0	2.74	-1.44	6.71	160 h
4	BL	0	4.17	-0.01	8.15	79 h

<sup>a</sup>Infection date  $\hat{u}'$  and its 95% confidence interval were calculated for each of the experimental sets in physiological time  $x'_k$  (equations 11–17). Determination was considered successful if computed interval contained the true infection date  $u'$  (i.e.,  $\hat{u}_{\text{lower}} < 0 < \hat{u}_{\text{upper}}$ ).

<sup>b</sup>Cultivar Basler Langstieler.

- sobstbau 1993. Eidg. Forschungsanstalt für Obst-, Wein- und Gartenbau, CH-8820 Wädenswil, Switzerland.
3. Batra, L. R. 1991. World Species of *Monilinia* (Fungi): Their Ecology, Biosystematics and Control. Mycologia Memoir No. 16. J. Cramer, Berlin.
  4. Baumgärtner, J., and Gutiérrez, A. P. 1989. Simulation techniques applied to pest and crop models. Boletín de sanidad vegetal. Fuera Ser. 17:175-214.
  5. Biggs, A. R., and Northover, J. 1988. Influence of temperature and wetness duration on infection of peach and sweet cherry fruits by *Monilinia fructicola*. Phytopathology 78:1352-1356.
  6. Brown, S. K., and Wilcox, W. F. 1989. Evaluation of cherry genotypes for resistance to fruit infection by *Monilinia fructicola*. HortScience 24:1013-1016.
  7. Bucksteeg, W. 1939. Untersuchungen über den Sporenflug bei Monilia als Grundlage für die chemische Bekämpfung. Z. Pflanzenkrankh. Pflanzenschutz 49:12-18.
  8. Byrde, R. J. W., and Willetts, H. J. 1977. The Brown Rot Fungi of Fruit: Their Biology and Control. Pergamon Press, Oxford.
  9. Campbell, C. L., and Madden, L. V. 1990. Introduction to Plant Disease Epidemiology. John Wiley & Sons, Inc., New York.
  10. Corbin, J. B., and Ogawa, J. M. 1974. Springtime dispersal patterns of *Monilinia laxa* conidia in apricot, peach, prune, and almond trees. Can. J. Bot. 52:167-176.
  11. Efron, B., and Tibshirani, R. J. 1993. An Introduction to the Bootstrap. Chapman and Hall, London.
  12. Fitt, B. D. L., McCartney, H. A., and Walklate, P. J. 1989. The role of rain in dispersal of pathogen inoculum. Annu. Rev. Phytopathol. 27:241-270.
  13. Höhn, H., and Siegfried, W. 1989. Aktuelles zum Pflanzenschutz im Obstbau. Schweiz. Z. Obst- und Weinbau 125:73-76.
  14. Jenkins, P. T. 1965. *Sclerotinia laxa* Aderh. & Ruhl.: A cause of brown-rot of stone fruits not previously recorded in Australia. Aust. J. Agric. Res. 16:141-144.
  15. Landgraf, F. A., and Zehr, E. I. 1982. Inoculum sources for *Monilinia fructicola* in South Carolina peach orchards. Phytopathology 72:185-190.
  16. Logan, J. A., Wollkind, D. J., Hoyt, S. C., and Tanigoshi, L. K. 1976. An analytic model for description of temperature dependent rate phenomena in arthropods. Environ. Entomol. 5:1133-1140.
  17. Manly, B. F. J. 1987. A multiple regression method for analysing stage-frequency data. Res. Popul. Ecol. 29:119-127.
  18. Mittmann-Maier, G. 1940. Untersuchungen über die *Monilia*-Resistenz von Sauerkirschen. Z. Pflanzenkrankh. 50:84-95.
  19. Ogawa, J. M., and English, H. 1960. Relative pathogenicity of two brown rot fungi, *Sclerotinia laxa* and *Sclerotinia fructicola*, on twigs and blossoms. Phytopathology 50:550-558.
  20. Richards, F. J. 1959. A flexible growth function for empirical use. J. Exp. Bot. 10:290-300.
  21. Rüegg, J., and Siegfried, W. 1993. Fruit production in Switzerland: Significance and control of disease caused by Monilia fungi. Pesticide Outlook 4 (2):15-18.
  22. Siegfried, W., Rüegg, J., and Grieder, E. 1990. Moniliajahr 1989. Unerwartet starkes Auftreten auf Kern- und Steinobst. Schweiz. Z. Obst- und Weinbau 126:126-133.
  23. Tamm, L., and Flückiger, W. 1993. Influence of temperature and moisture on growth, spore production, and conidial germination of *Monilinia laxa*. Phytopathology 83: 1321-1326.
  24. Wilcox, W. F. 1989. Influence of environment and inoculum density on the incidence of brown rot blossom blight of sour cherry. Phytopathology 79:530-534.
  25. Zbinden, W. 1986. Die Moniliakrankheit bei der Süsskirsche, Beobachtungen aus der Praxis. Schweiz. Z. Obst- und Weinbau 122:247-248.
  26. Zwygart, T. 1970. Untersuchungen über Wirt-Parasit-Beziehungen bei Moniliosen an Obstbäumen. Phytopathol. Z. 68:97-130.